Journal of Hazardous Materials 190 (2011) 566–573

Contents lists available at ScienceDirect

Journal of Hazardous Materials

journal homepage: www.elsevier.com/locate/jhazmat

Hydrothermal growth of nanometer- to micrometer-size anatase single crystals with exposed (0 0 1) facets and their ability to assist photodegradation of rhodamine B in water

Jin-Ming Wu*, Mei-Lan Tang

State Key Laboratory of Silicon Materials, Zhejiang University, Zheda Road 38#, Hangzhou 310027, PR China

ARTICLE INFO

Article history:
Received 16 December 2010
Received in revised form 18 March 2011
Accepted 22 March 2011
Available online 29 March 2011

Keywords:
Nanostructure
Titanium oxide
Hydrothermal synthesis
Single crystal

ABSTRACT

Anatase single crystals with exposed (0 0 1) facets have been the focus of many researches in recent years. This paper reports the hydrothermal synthesis of (0 0 1)-exposed anatase single crystals through reactions of Ti plates in aqueous HF solutions with mass concentrations of 0.15–0.80%, in an autoclave at 180 °C for 2–12 h. The size of the achieved anatase single crystals varied from 0.4 to 13.6 μm, exposing 15–49% (0 0 1) facets. The crystal size and the (0 0 1) fraction increased with increasing HF concentrations. For a prolonged reaction time, anatase crystals with larger sizes and reduced fractions of (0 0 1) facets were achieved. The activity of the anatase crystals to assist photodegradation of rhodamine B in water increased with decreasing sizes and increasing fractions of (0 0 1) facets. Selective erosion of the anatase single crystals along the high-energy (0 0 1) facets was noted, for the first time, which resulted in cone-shaped walls with a thickness ranging from several to hundreds of nanometers. The selective erosion contributed to the photocatalytic activity of the (0 0 1)-exposed anatase single crystals.

1. Introduction

Titania (TiO_2) is the most commonly studied semiconductor to assist photodegradation of organic pollutants in wastewater [1]. Due to the relatively high density of unsaturated 5-fold Ti and the unique electronic structure, the (0 0 1) surface of anatase TiO_2 has been argued theoretically to possess a photocatalytic activity advantageous over the thermodynamic stable (1 0 1) one [2,3]. Yang et al. synthesized, for the first time, single-crystalline anatase with 47% {0 0 1} facets through hydrothermally heating a mixed aqueous solution of TiF_4 and HF, where the selective absorption of F^- stabilizes the high-energy {0 0 1} facets [4]. With the help of 2-propanol, the percentage of {0 0 1} facets was later improved to 64%, and the achieved anatase crystals were reported to generate more active hydroxyl radicals (•OH) upon UV irradiation when compared to the commercial Degussa P25 titania nanoparticles, in spite of the much smaller specific surface area (1.6 and 47.0 m^2/g for anatase crystals and P25, respectively) [5]. Since then, anatase crystals with various percentages of exposed {0 0 1} facets have been reported in the nearest two years [6–15]. Most of the anatase crystals achieved till now are ca. 1 μm in size. What is of interest is the scale-down of the single crystals [9,11], which contributes to an enhanced specific surface area as well as a reduced migration path for the photogenerated charges to the surface to be involved in a photocatalytic reaction. On the other hand, to be used as model crystals for fundamental studies in surface science, large anatase single crystals with exposed (0 0 1) facets are also of great interest [14].

Most of the (0 0 1)-exposed anatase crystals above-mentioned are powders; yet for wastewater treatments, the usage of immobilized catalysts is advocated because it avoids the subsequent catalysts-recovery procedure involved in a slurry system [16]. A reduced catalyst–reactant contacting opportunity decreases the catalytic efficiency for the immobilized system; however, developments in photoreactor designs alleviate to some extent such a shortcoming. For example, a rotating disk reactor designed by Dionysiou et al. achieved an efficiency similar to that of a generally adopted slurry system [17]. Therefore, it is desirable to fabricate titania films with high photocatalytic activity.

Photocatalytically active titania films can be fabricated by direct oxidation of metallic Ti substrates through various approaches of anodic oxidations [18], H_2O_2-treatments [19], alkali-thermal treatments [20], HF-treatments [7], and thermal oxidations in an atmosphere of acetone [21] or ethanol [22]. In this paper, we reported the hydrothermal growth of anatase single crystals immobilized on Ti substrates. For the first time, anatase single crystals with controlled sizes ranging from 0.4 to 14 μm (the largest crystals reported till now) and fractions of (0 0 1) facets ranging from 15% to 49% were fabricated through fine-tuning the reaction parame-

* Corresponding author. Tel.: +86 571 87953115; fax: +86 571 87953115.
E-mail address: msewjm@zju.edu.cn (J.-M. Wu).

0304-3894/$ – see front matter © 2011 Elsevier B.V. All rights reserved.
doi:10.1016/j.jhazmat.2011.03.079

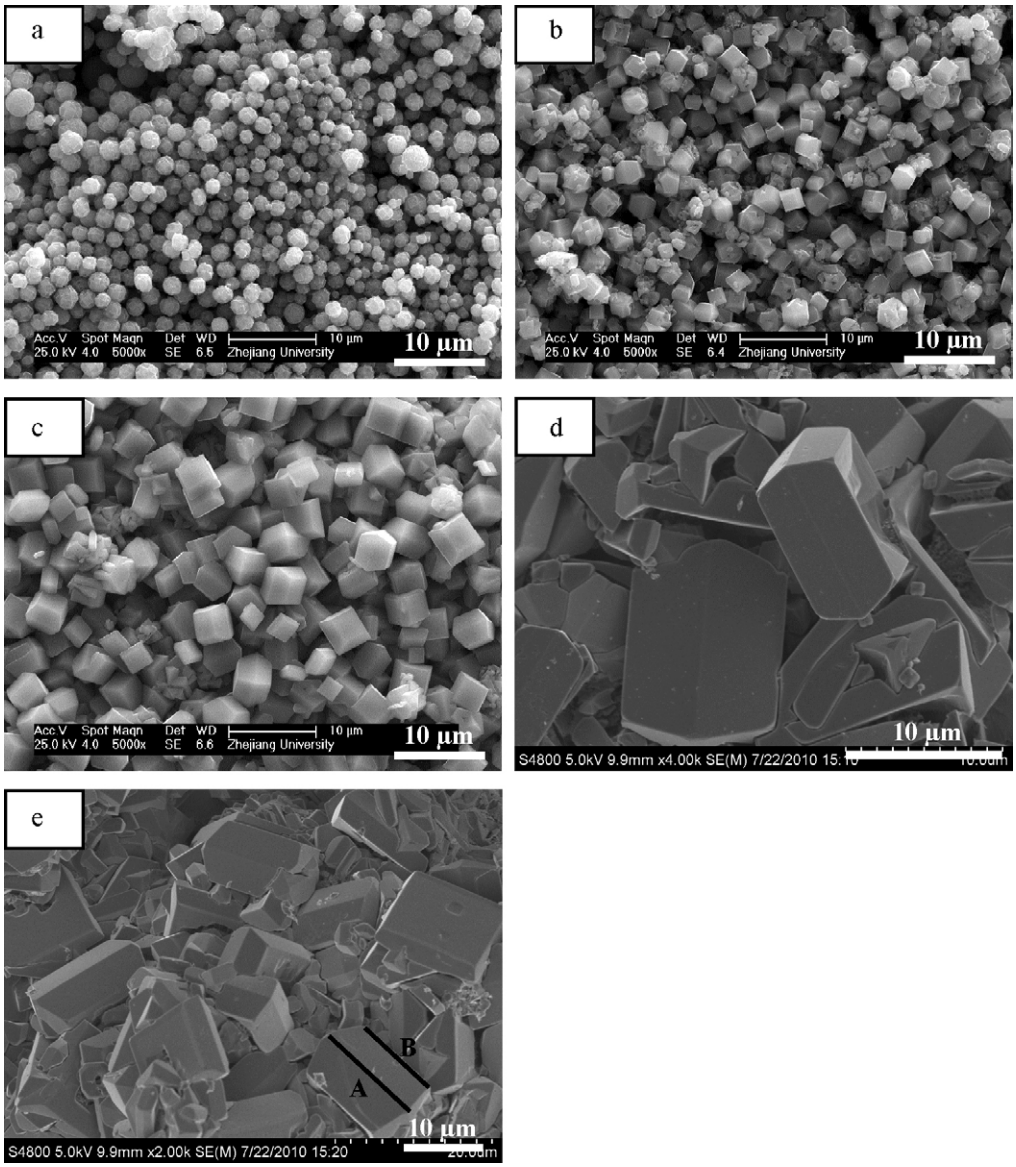

Fig. 1. FE-SEM surface morphologies of Ti plates after the hydrothermal treatments at 180 °C for 12 h in aqueous HF solutions with a mass concentration of (a) 0.10%, (b) 0.15%, (c) 0.20%, (d) 0.40% and (e) 0.80%.

ters. The ability of the immobilized anatase single crystals to assist photodegradation of rhodamine B, a typical azo dye, was evaluated and related to the crystal size and the fraction of {0 0 1} facets.

2. Experimental procedure

Pieces of Ti specimens with sizes of 2 cm × 2 cm × 0.2 cm were cut from a sheet of commercial pure titanium (TA2) with the purity of 99.8%. They were etched in a 1:3:6 (in volume) mixture of a 55 mass% HF aqueous solution, a 63 mass% HNO_3 aqueous solution and distilled water for 2 min, followed by ultrasonic cleaning. Each Ti plate was immersed in 45 mL HF aqueous solution with a mass concentration of 0.10–0.80%, which was then sealed tightly in a Teflon-lined autoclave (50 mL in volume) and kept for 1–24 h in an oven maintained at 180 °C. The Ti plate after the reaction was then rinsed gently in distilled water and dried at 80 °C before further characterizations.

The surface morphology was examined using a field emission scanning electron microscopy (FE-SEM, Hitachi S-4800, Tokyo, Japan). The high-resolution transmission electron microscopy (HR-TEM) examination was conducted employing a JEM-2010 microscopy (JEOL, Japan) working at 200 kV. To prepare the samples for TEM characterizations, anatase crystals were detached off from the reacted Ti plate and then placed on a carbon pre-coated copper grid. The X-ray diffraction (XRD) tests were performed using a Rigaku D/max-3B diffractometer (Tokyo, Japan) with CuKα radiation, operated at 40 kV, 36 mA (λ = 0.154056 nm). UV–Vis diffuse reflectance spectra were collected using a UV–Vis near-infrared spectrometer (UV-3150, Shimadzu, Japan).

Photocatalytic activity was evaluated using 20 mL rhodamine B aqueous solution with an initial concentration of 0.005 mM. The illumination of the immobilized titania layer ($2 \times 2\,cm^2$ in area) was provided by a 20 W UV lamp with the maximum radiation at 365 nm. The lamp was kept ca. 4 cm over the solution and the average intensity of UV irradiance reaching the sample was measured to be ca. 2.2 mW/cm^2, using a UV-A irradiance meter (Beijing Normal University, China, measured for the wavelength range of 320–400 nm with a peak wavelength of 365 nm). The solution was stirred continuously and exposed to air during the photocatalytic reaction. A schematic image showing the setup of the

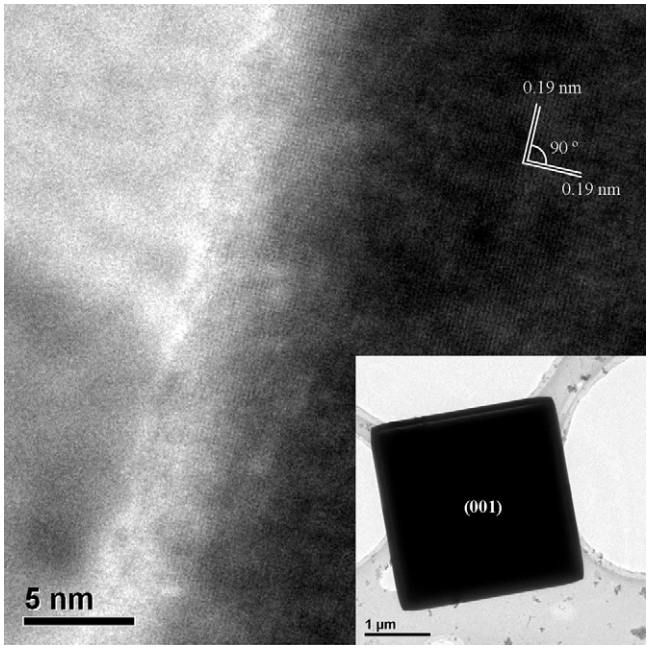

Fig. 2. HR-TEM image of a (0 0 1)-exposing anatase single-crystallite scratched off from the Ti plate subjected to hydrothermal treatment in 0.2% HF at 180 °C for 12 h. Inset shows the corresponding low-magnification image.

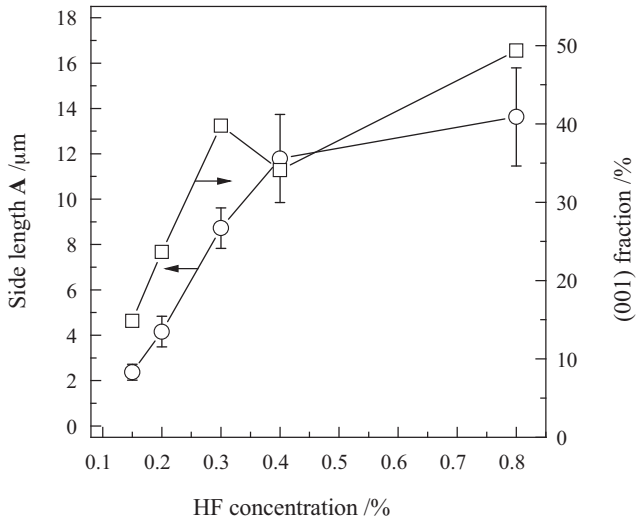

Fig. 3. Changes in the size and the percentage of (0 0 1) facets of the separated truncated bipyramids as a function of the HF concentration. The error bar represents the standard deviation of the longer side length from ten selected truncated bipyramids.

photocatalytic reaction can be found in Scheme 1 in the Supporting Information. The change in the rhodamine B concentration was monitored with a UV–Vis spectrophotometer (UV-1800PC, Shanghai Mapada, Shanghai, China) at a wavelength of 553 nm, using a quartz cuvette of 1 cm of the optical path length. For comparison in photocatalytic activity, titania layers consisted of Degussa P25 nanoparticles on Ti substrates were also prepared following a procedure described elsewhere [23,24]. The layer thickness was kept constant at ca. 3 μm.

3. Results

Fig. 1 shows surface morphologies of Ti plates after the hydrothermal treatment at 180 °C for 12 h in aqueous HF solutions with various concentrations. When the HF concentration was maintained at 0.10%, homogeneously dispersed multi-facet microspheres with sizes of ca. 1–2 μm were achieved. The spheres consisted of anatase single crystals looking like truncated bipyramids (Fig. 1a), with (0 0 1) facets exposed outside [7]. When the HF concentration increased to 0.15% (Fig. 1b) and 0.20% (Fig. 1c), highly truncated bipyramids appeared on the Ti plates except for the multi-facet microspheres. The bipyramids are almost the same in morphology with those obtained by Yang et al. [5]. It can be seen clearly that each truncated bipyramid possesses two parallel {0 0 1} facets and eight {1 0 1} facets. Fig. S1 in the Supporting Information demonstrates the FE-SEM observation of the sample derived utilizing 0.20% HF in details. The separated truncated bipyramids, which are quite homogeneous in size, can be seen covering thoroughly the Ti plate. When the HF concentration further increased to a value beyond 0.40%, most of the truncated bipyramids interlocked with each other and several defects on the (0 0 1) facet can be discerned (Fig. 1d and e).

Fig. 2 illustrates the HR-TEM image of a single-crystallite scratched off from the Ti plate subjected to the hydrothermal treatment in 0.20% HF at 180 °C for 12 h. The perpendicular lattice with a space of 0.19 nm corresponds well to the (2 0 0) and (0 2 0) atomic planes of the anatase TiO_2. Therefore, the HR-TEM analysis confirms that the two parallel faces of the anatase crystal are (0 0 1) facets.

Fig. 3 shows the statistical size (defined as side length A as illustrated in Fig. 1e) and the calculated percentage of (0 0 1) facets of the separated truncated bipyramids as a function of the HF concentration. The details for the statistic and calculation can be found in Fig. S2 in the Supporting Information. With increasing HF concentrations from 0.15% to 0.40%, the average size of truncated bipyramids increased almost linearly from 2.4 to 11.8 μm. Further increasing the HF concentration to 0.80% resulted in truncated bipyramids with an average size of ca. 13.6 μm, which is the largest one among those reported, to the best of our knowledge. The fraction of (0 0 1) facets increased from 15% to 40% with increasing HF concentrations from 0.15% to 0.30%, which reached at 49% when 0.80% HF was used.

Fig. 4 demonstrates the change in surface morphology for the Ti plate subjected to hydrothermal treatments in 0.20% HF for various durations. The heavy corrosion of the Ti plate, together with some irregular precipitates on the surface, was significant for the initial reaction of 1 h (Fig. 4a). Both multi-facet microspheres and separated truncated bipyramids were seen covering the Ti plate after 2 h reaction (Fig. 4b). For further prolonged reaction durations, the separated truncated bipyramids predominated gradually the surface of Ti plates over the multi-facet microspheres (comparing Fig. 4c and d and Fig. 1c). Fig. 5 shows that, the separated truncated bipyramids grew to give an average size of ca. 4.4 μm with increasing reaction time to 6 h. The size remained almost unchanged with further prolonged durations. The fraction of (0 0 1) facets, on the contrary, decreased with increasing reaction time. It is interesting to find that almost all the truncated bipyramids achieved after 24 h reaction have been selectively eroded. Close observations on a thoroughly eroded truncated bipyramid as shown in Fig. 4f suggest that the (0 0 1) facets of truncated bipyramids have been selectively eroded; therefore, the real fraction of (0 0 1) facets is far below the calculated value of 18% as illustrated in Fig. 5. In addition, the surface of Ti plates after 24 h reaction became rough. Large aggregations consisted of interlocked truncated bipyramids that have been eroded can also be found on Ti surfaces (see Fig. S3 in the Supporting Information).

Fig. 6 illustrates a cross-sectional image of the titania layer derived by the hydrothermal treatment of a Ti plate in 0.20% HF at 180 °C for 12 h. The film thickness was estimated roughly to be over 100 μm. A close observation on the fracture surface reveals titania with morphologies of both multi-facet microspheres and separated

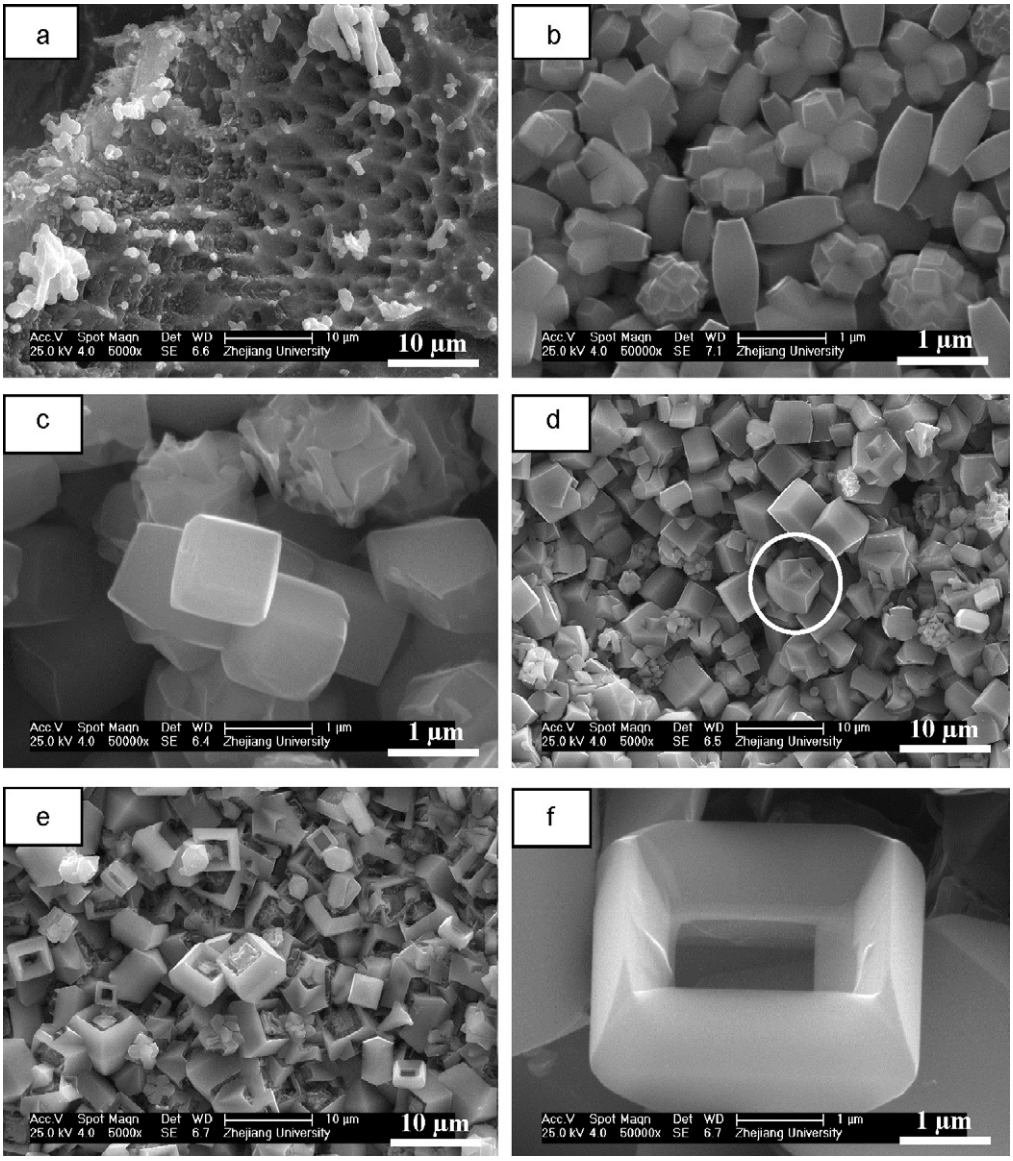

Fig. 4. FE-SEM surface morphologies of Ti plates after the hydrothermal treatments in 0.20 mass% HF at 180 °C for (a) 1 h, (b) 2 h, (c) 3 h, (d) 6 h, (e) and (f) 24 h.

truncated bipyramids. Although the top-view image shows that the separated truncated bipyramids predominate over the microspheres, the amounts of the truncated bipyramids are relatively less on the fracture surface.

Fig. 7 indicates the XRD patterns of the Ti plate after the hydrothermal treatment in 0.20% HF at 180 °C for 3, 12 and 24 h. All the three patterns fitted well to the standard card JCPDS 21-1272 corresponding to anatase, suggesting a high phase purity for the achieved titania. The sharp XRD peaks suggest that anatase crystals were well crystallized. Because of the random distribution of the truncated bipyramids, no enhanced intensity for the XRD peak corresponding to anatase (0 0 4), which locates at 37.8° in 2θ, can be discerned.

The UV–Vis diffuse reflectance spectra of two immobilized anatase layers obtained by hydrothermal treatments of Ti plates at 180 °C for 12 h in aqueous HF with concentrations of 0.15 and 0.20%, respectively, are demonstrated in Fig. 8. Here, the samples were subjected to a subsequent calcination in air at 450 °C for 1 h. The sample achieved using 0.15% HF, which exhibited smaller crystal size as well as lower (0 0 1) fraction, possessed relatively a lower reflectance in UV region and higher reflectance in visible region. Assuming an indirect transition between bands, the band gap of titania can be estimated applying a well-established method [24]. The estimated band gap for the two samples derived using 0.15% and 0.20% HF are quite similar (3.15 and 3.10 eV, respectively), which is in good accordance to that of bulk anatase.

Fig. 9a illustrates the photodegradation curves of rhodamine B in water in the presence of the as-synthesized single-crystalline anatase layer derived by hydrothermal treatments of Ti plates in 0.20 mass% HF at 180 °C for 3, 12 and 24 h. All the three curves can be fitted to a straight line passing through the zero in the $\ln(c_0/c) \sim t$ plot, suggesting that the photodegradation reaction was a pseudo-first order one. Here, c and c_0 denote the rhodamine B concentration before and after the reaction, and t is the illumination time. The reaction rate constant, which can be derived by the slope of the straight lines shown in Fig. 9b, was 5.5, 4.8 and 6.6×10^{-3} min^{-1}, respectively, for the three immobilized anatase layers derived by the hydrothermal reactions for 3, 12 and 24 h.

Fig. 10 shows the photodegradation curves of rhodamine B in water in the presence of the immobilized single-crystalline anatase layers derived by hydrothermal treatments of Ti plates at 180 °C for 12 h in aqueous HF with various mass concentrations of 0.15, 0.20

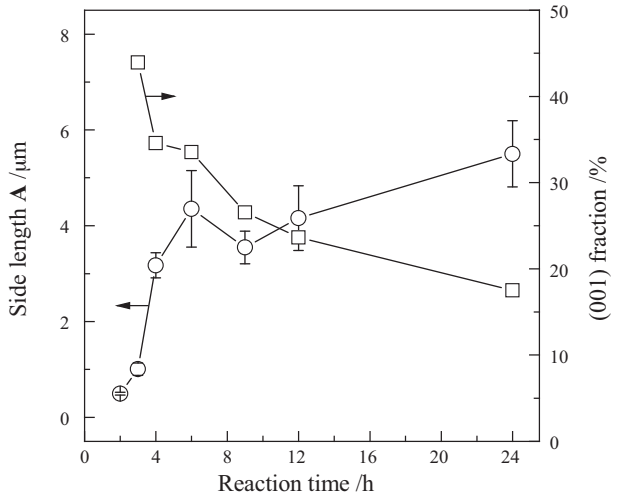

Fig. 5. The size and the percentage of (0 0 1) facets of the separated truncated bipyramids derived by hydrothermally heating a Ti plate in 0.2% HF at 180 °C for various durations. The error bar represents the standard deviation of the longer side length from ten selected truncated bipyramids.

and 0.40%, after a subsequent calcination at 450 °C for 1 h. For comparison, that assisted with the layer consisted of P25 nanoparticles is also illustrated. The slopes in Fig. 10b gave reaction rate constants of 8.7, 7.1 and 7.1×10^{-3} min^{-1}, respectively, for the three layers derived using 0.15, 0.20 and 0.40% HF. The P25 layer exhibited a reaction rate constant of 7.9×10^{-3} min^{-1}. For the layer obtained using 0.20% HF at 180 °C for 12 h, it is clear that the subsequent calcination improved significantly the reaction rate constant from 4.8 to 7.1×10^{-3} min^{-1}, which can be contributed to the removal of F atoms incorporated in titania [25,26]. The photocatalytic activity decreased with increasing HF concentration from 0.15 to 0.20%, which then remained unchanged for a further increasing HF concentration to 0.40%. The activity of the later two samples to assist photodegradation of rhodamine B in water is slightly lower than that of P25. It is noted that, the P25 layer possessed a thickness of only 3 μm, which is much thinner than that of the immobilized single-crystalline anatase layers derived in the current investigation. However, the present comparison in photocatalytic activity is reasonable because photodegradation reactions occur mainly on the surface. A film thickness beyond 3 μm is enough to make full use of the light provided with a UV lamp [27]. As a support, the UV–Vis diffuse reflectance spectrum reported previously [24] suggested that the P25 layer with a film thickness of ca. 3 μm absorbs nearly 95% UV light, which is even higher than the UV absorbance of ca. 90% for the present anatase layers (Fig. 8).

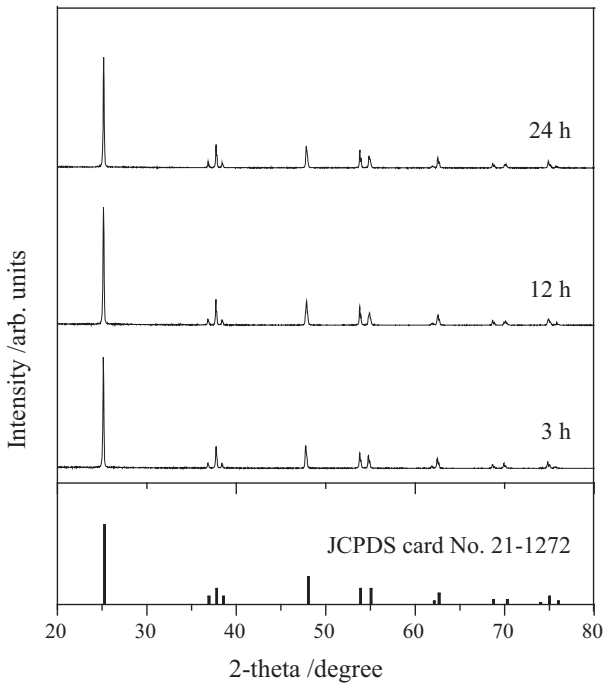

Fig. 7. XRD patterns of the immobilized anatase layer obtained by hydrothermally heating Ti plates in 0.20 mass% HF at 180 °C for 3, 12 and 24 h.

4. Discussion

The possible reactions involved in the Ti–HF interactions under a hydrothermal condition include [28],

$$Ti + 6HF \rightarrow H_2TiF_6 + 2H_2\uparrow \quad (1)$$

$$H_2TiF_6 + 4H_2O \rightarrow Ti(OH)_4 + 6HF \quad (2)$$

$$Ti(OH)_4 \rightarrow TiO_2\downarrow + 2H_2O \quad (3)$$

Anatase nanocrystals shaped as truncated bipyramids are generally achieved in such a HF-mediated synthesis [29]. In the current investigation, HF acts as a corrosive to attack the Ti plate to release finally Ti(IV)-hydrates into the reactants for titania precipitations; at the same time, the selective absorption of F^- ions on the (0 0 1) facets of anatase crystals achieved the formation of truncated bipyramids. The increasing HF concentration not only resulted in more Ti(IV)-hydrates in solutions, but also enhanced retarding effects for the vanish of facets other than (0 0 1) during the crystal growth; therefore, it is not surprising that an increasing HF concen-

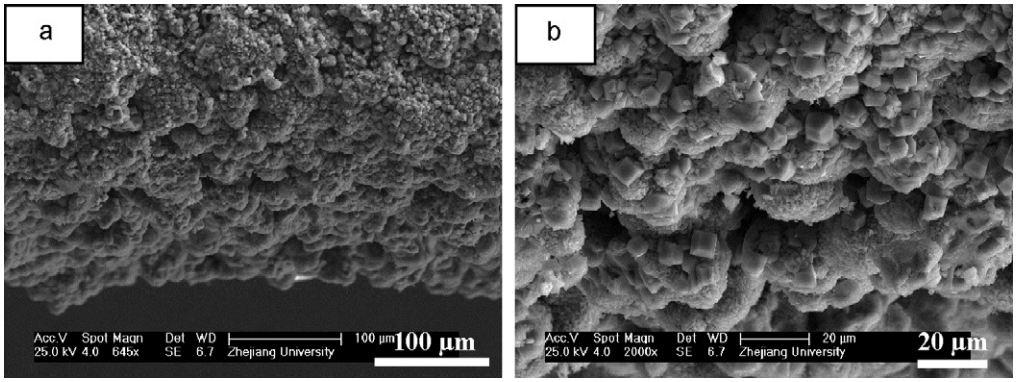

Fig. 6. FE-SEM cross-sectional images with (a) low and (b) high magnifications of the immobilized anatase layer derived by hydrothermally heating a Ti plate in 0.20 mass% HF at 180 °C for 12 h.

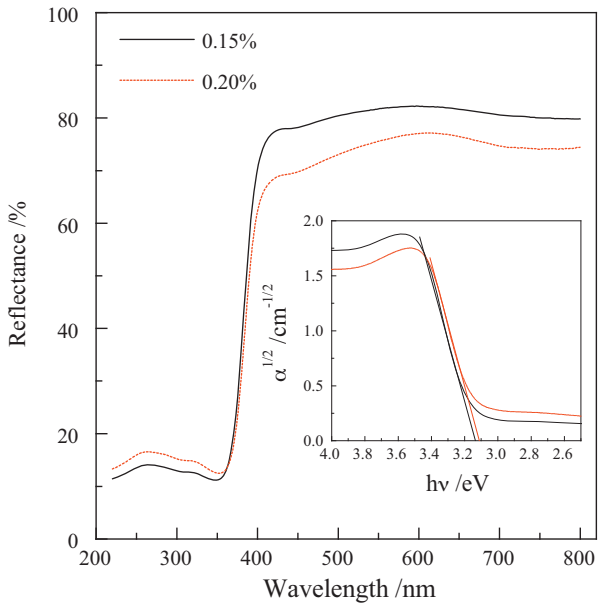

Fig. 8. UV–Vis diffuse reflectance of the immobilized anatase layer obtained by hydrothermally treating Ti plates at 180 °C for 12 h in aqueous HF with concentrations of 0.15 and 0.20%, followed by a subsequent calcination in air at 450 °C for 1 h. Re-plotting of the curve in the $\alpha^{1/2} \sim h\nu$ coordinate (inset) gives the corresponding band gap, assuming an indirect transition between bands for titania.

tration favored the growth of larger anatase single crystals with the shape of highly truncated bipyramids (Fig. 3).

Eqs. (1)–(3) suggest that, in theory, the amount of F^- ions in the solution remains unchanged during the reaction. However, during the growth of the truncated bipyramids, more and more F^- ions are absorbed on the anatase crystals. As a result, for the anatase crystals grown at the later stage of the reaction, the density of F^- ions on the (0 0 1) facets reduced. Therefore, as illustrated in Fig. 5, although the crystal size further increased, the fraction of (0 0 1) facets for the anatase crystals decreased with increasing reaction time due to the reduced retarding effect arising from the selective absorption of F^- ions on the (0 0 1) facets.

Till now, no reports appeared on the corrosion of the separated anatase truncated bipyramids by HF. Actually, with a prolonged duration beyond 24 h, the erosion of precipitated anatase single crystals with HF is possible under the hydrothermal condition according to the followed reaction [28],

$$TiO_2 + 6HF \rightarrow H_2TiF_6 + 2H_2O \quad (4)$$

The absorption of F^- ions on the (0 0 1) facets of anatase single crystals stabilized the high-energy facet. However, when the precipitated anatase crystals were maintained under the hydrothermal condition for a duration long enough, the selective erosion of the high-energy (0 0 1) facets by HF molecules did occur, as indicated clearly in Fig. 4.

During the crystal growth, when a separated truncated bipyramid is eroded by HF to introduce some defects on the surface, the heterogeneous nucleation of a secondary bipyramid on the defect is possible, which leads to the typical intermediate morphology as circled in Fig. 4d. The continuous nucleation and growth of the truncated bipyramids on the primary one achieved finally the multi-facet spheres as demonstrated in Fig. 1a. In the current investigation, there exists a competition in the growth of multi-facet spheres and separated truncated bipyramids. A high HF concentration beyond 0.15% favored the formation of the separated truncated bipyramids. It seems that a high supersaturation with respect to titania, which resulted from high HF concentrations, favors the homogeneous nucleation and the subsequent growth of anatase single crystals. This in turn results in more separated truncated bipyramids.

Comparing the three as-synthesized anatase layers synthesized at 180 °C for various durations utilizing 0.20% HF (Fig. 9), it can be seen that the 3h-derived immobilized anatase layer exhibited a photocatalytic activity higher than the one obtained by 12 h reaction. This can be contributed to two factors, that is, significantly smaller size and higher fraction of (0 0 1) facets (Fig. 5). However, for the three as-synthesized anatase layers, the one fabricated by 24 h reaction possessed the best activity. The anatase single crystals with more exposed (0 0 1) facets have been proved to exhibit higher photocatalytic activity [5,7,12–15]. For the anatase layer obtained by 24 h reaction, most of the (0 0 1) facets were selectively eroded, which should have led to a reduced activity. However, the selective erosion resulted in cone-shaped walls with thickness ranged from several to hundreds of nanometers (Fig. 4e and f). The single-crystalline nature of titania favors the migration of photogenerated electron-hole pairs [30,31]. Such a positive effect will be enhanced in case that the charge migration path is reduced. Therefore, the selectively eroded anatase single crystals exhibited the best photocatalytic activity among the three, in spite of the much-reduced fraction of (0 0 1) facets.

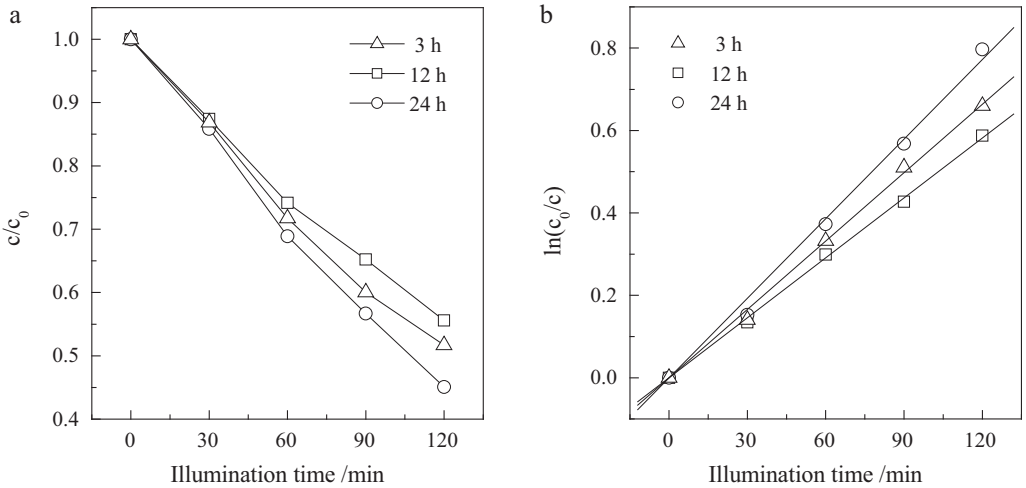

Fig. 9. Photodegradation of rhodamine B in water in the presence of the as-synthesized anatase layer derived by hydrothermally treating Ti plates in 0.20 mass% HF at 180 °C for 3, 12 and 24 h: (a) the degradation curve and (b) the fitting result assuming a pseudo-first order reaction.

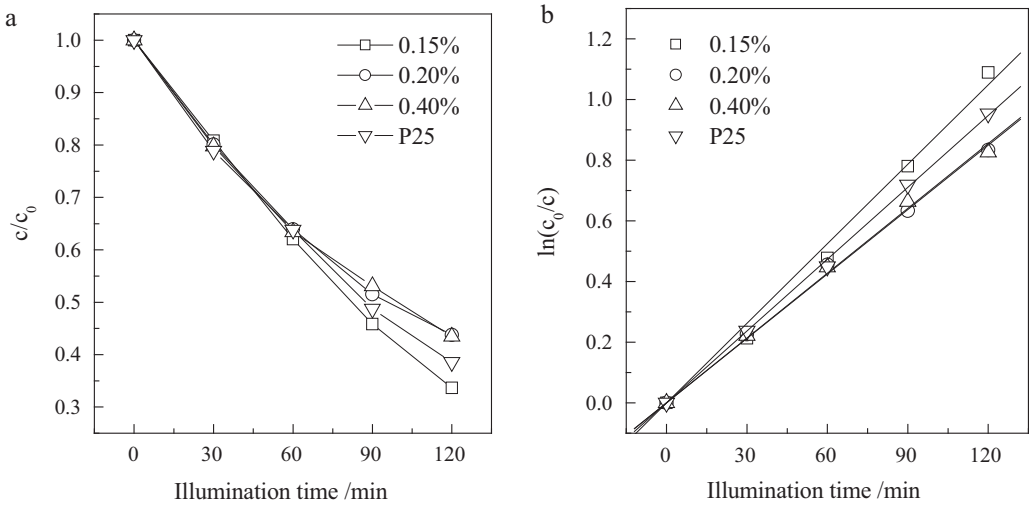

Fig. 10. Photodegradation of rhodamine B in water in the presence of the immobilized anatase layer derived by hydrothermally treating Ti plates at 180 °C for 12 h in aqueous HF with various concentrations of 0.15, 0.20 and 0.40%, followed by a subsequent calcination in air at 450 °C for 1 h: (a) the degradation curve and (b) the fitting result assuming a pseudo-first order reaction. Those derived utilizing immobilized P25 titania nanoparticles are also provided as a reference.

After the subsequent calcination, the anatase layer synthesized at 180 °C for 12 h using 0.15% HF exhibited higher photocatalytic activity than those derived using 0.20% and 0.40% HF (Fig. 10). Considering that the former possessed smaller size but lower fraction of (0 0 1) facets (Fig. 3), it concludes that the crystal size affects more significantly the photocatalytic activity when compared with the (0 0 1) fraction. The higher absorption in UV light for the 0.15% HF-derived sample (Fig. 8) also contributed to its higher photocatalytic activity.

5. Conclusions

Anatase single crystals have been fabricated through hydrothermal treatments of Ti plates in aqueous HF solutions at 180 °C. The crystals look like highly truncated bipyramids, with sizes ranging from 0.4 to 13.6 μm and (0 0 1) fractions ranging from 15% to 49%. Both the crystal size and the (0 0 1) fraction increased with increasing HF concentrations from 0.15% to 0.80%; whereas the prolonged reaction time for up to 12 h in 0.20% HF resulted in larger anatase crystals with reduced fractions of (0 0 1) facets. The activity of the immobilized anatase layers to assist photodegradation of rhodamine B in water increased with increasing fractions of (0 0 1) facets and decreasing crystal sizes. The size affects more significantly the photocatalytic activity. With a prolonged reaction time to 24 h in 0.20% HF, the selective erosion of the anatase truncated bipyramids along the high-energy (0 0 1) facets occurred. As a result, cone-shaped walls with a thickness ranging from several to hundreds of nanometers were obtained, which contributes to the photocatalytic activity.

Acknowledgement

This work is supported by Zhejiang Provincial Natural Science Foundation (project no. Y4080001).

Appendix A. Supplementary data

Supplementary data associated with this article can be found, in the online version, at doi:10.1016/j.jhazmat.2011.03.079.

References

[1] X. Chen, S.S. Mao, Titanium dioxide nanomaterials: synthesis, properties, modifications, and applications, Chem. Rev. 107 (2007) 2891–2959.
[2] X.Q. Gong, A. Selloni, Reactivity of anatase TiO_2 nanoparticles: the role of the minority (0 0 1) surface, J. Phys. Chem. B 109 (2005) 19560–19562.
[3] X.Q. Gong, A. Selloni, M. Batzill, U. Diebold, Steps on anatase TiO_2 (1 0 1), Nat. Mater. 5 (2006) 665–670.
[4] H.G. Yang, C.H. Sun, S.Z. Qiao, J. Zou, G. Liu, S.C. Smith, H.M. Cheng, G.Q. Lu, Anatase TiO_2 single crystals with a large percentage of reactive facets, Nature 453 (2008) 638–644.
[5] H.G. Yang, G. Liu, S.Z. Qiao, C.H. Sun, Y.G. Jin, S.C. Smith, J. Zou, H.M. Cheng, G.Q. Lu, Solvothermal synthesis and photoreactivity of anatase TiO_2 nanosheets with dominant {0 0 1} facets, J. Am. Chem. Soc. 131 (2009) 4078–4083.
[6] J.G. Yu, J.J. Fan, K.L. Lv, Anatase TiO_2 nanosheets with exposed (0 0 1) facets: improved photoelectric conversion efficiency in dye-sensitized solar cells, Nanoscale 2 (2010) 2144–2149.
[7] M. Liu, L.Y. Piao, W.M. Lu, S.T. Ju, L. Zhao, C.L. Zhou, H.L. Li, W.J. Wang, Flower-like TiO_2 nanostructures with exposed {0 0 1} facets: facile synthesis and enhanced photocatalysis, Nanoscale 2 (2010) 1115–1117.
[8] J.S. Chen, Y.L. Tan, C.M. Li, Y.L. Cheah, D.Y. Luan, S. Madhavi, F.Y.C. Boey, L.A. Archer, X.W. Lou, Constructing hierarchical spheres from large ultrathin anatase TiO_2 nanosheets with nearly 100% exposed (0 0 1) facets for fast reversible lithium storage, J. Am. Chem. Soc. 132 (2010) 6124–6130.
[9] Y.Q. Dai, C.M. Cobley, J. Zeng, Y.M. Sun, Y.N. Xia, Synthesis of anatase TiO_2 nanocrystals with exposed {0 0 1} facets, Nano Lett. 9 (2009) 2455–2459.
[10] H. Ariga, T. Taniike, H. Morikawa, M. Tada, B.K. Min, K. Watanabe, Y. Matsumoto, S. Ikeda, K. Saiki, Y. Iwasawa, Surface-mediated visible-light photo-oxidation on pure TiO_2 (0 0 1), J. Am. Chem. Soc. 131 (2009) 14670–14671.
[11] X.G. Han, Q. Kuang, M.S. Jin, Z.X. Xie, L.S. Zheng, Synthesis of titania nanosheets with a high percentage of exposed (0 0 1) facets and related photocatalytic properties, J. Am. Chem. Soc. 131 (2009) 3152–3153.
[12] G. Liu, H.G. Yang, X.W. Wang, L.N. Cheng, J. Pan, G.Q. Lu, H.M. Cheng, Visible light responsive nitrogen doped anatase TiO_2 sheets with dominant {0 0 1} facets derived from TiN, J. Am. Chem. Soc. 131 (2009) 12868–12869.
[13] S.W. Liu, J.G. Yu, M. Jaroniec, Tunable photocatalytic selectivity of hollow TiO_2 microspheres composed of anatase polyhedra with exposed {0 0 1} facets, J. Am. Chem. Soc. 132 (2010) 11914–11916.
[14] D.Q. Zhang, G.S. Li, X.F. Yang, J.C. Yu, A micrometer-size TiO_2 single-crystal photocatalysts with remarkable 80% level of reactive facets, Chem. Commun. 29 (2009) 4381–4383.
[15] Q.J. Xiang, K.L. Lv, J.G. Yu, Pivotal role of fluorine in enhanced photocatalytic activity of anatase TiO_2 nanosheets with dominant (0 0 1) facets for the photocatalytic degradation of acetone in air, Appl. Catal. B 96 (2010) 557–564.
[16] T.V. Gerven, G. Mul, J. Moulijn, A. Stankiewicz, A review of intensification of photocatalytic processes, Chem. Eng. Process. 46 (2007) 781–789.
[17] D.D. Dionysiou, G. Balasubramanian, M.T. Suidan, A.P. Khodadoust, I. Baudin, M. Laine, Rotating disk photocatalytic reactor: development, characterization, and evaluation for the destruction of organic pollutants in water, Water Res. 34 (2000) 2927–2940.
[18] Z.H. Zhang, Y. Yuan, L.H. Liang, Y.X. Cheng, G.Y. Shi, L.T. Jin, Preparation and photoelectrocatalytic activity of ZnO nanorods embedded in highly ordered TiO_2 nanotube arrays electrode for azo dye degradation, J. Hazard. Mater. 158 (2008) 517–522.

[19] J.M. Wu, B. Qi, Low-temperature growth of a nitrogen-doped titania nanoflower film and its ability to assist photodegradation of rhodamine B in water, J. Phys. Chem. C 111 (2007) 666–673.
[20] F.D. Mai, W.L.W. Lee, J.L. Chang, S.C. Liu, C.W. Wu, C.C. Chen, Fabrication of porous TiO_2 film on Ti foil by hydrothermal process and its photocatalytic efficiency and mechanisms with ethyl violet dye, J. Hazard. Mater. 177 (2010) 864–875.
[21] X.S. Peng, A.C. Chen, Aligned TiO_2 nanorod arrays synthesized by oxidizing titanium with acetone, J. Mater. Chem. 14 (2004) 2542–2548.
[22] S. Daothong, N. Songmee, S. Thongtem, P. Singjai, Size-controlled growth of TiO_2 nanowires by oxidation of titanium substrates in the presence of ethanol vapor, Scripta Mater. 57 (2007) 567–570.
[23] J.M. Wu, H.X. Xue, Photocatalytic active titania nanowire arrays on Ti substrates, J. Am. Ceram. Soc. 92 (2009) 2139–2143.
[24] X.M. Song, J.M. Wu, M. Yan, Photocatalytic degradation of selected dyes by titania thin films with various nanostructures, Thin Solid Films 517 (2009) 4341–4347.
[25] X.M. Song, J.M. Wu, M. Yan, Photocatalytic and photoelectrocatalytic degradation of aqueous rhodamine B by low-temperature deposited anatase thin films, Mater. Chem. Phys. 112 (2008) 510–515.
[26] J.M. Wu, B. Huang, Y.H. Zeng, Low-temperature deposition of anatase thin films on titanium substrates and their abilities to photodegrade Rhodamine B in water, Thin Solid Films 497 (2006) 292–298.
[27] A. Mills, G. Hill, S. Bhopal, I.P. Parkin, S.A. O'Neill, Thick titanium dioxide films for semiconductor photocatalysis, J. Photochem. Photobiol. A: Chem. 160 (2003) 185–194.
[28] G.S. Wu, J.P. Wang, D.F. Thomas, A.C. Chen, Synthesis of F-doped flower-like TiO_2 nanostructures with high photoelectrochemical activity, Langmuir 24 (2008) 3503–3509.
[29] K.L. Ding, Z.J. Miao, B.J. Hu, G.M. An, Z.Y. Sun, B.X. Han, Z.M. Liu, Shape and size controlled synthesis of anatase nanocrystals with the assistance of ionic liquid, Langmuir 26 (2010) 5129–5134.
[30] X.M. Song, J.M. Wu, M.Z. Tang, B. Qi, M. Yan, Enhanced photoelectrochemical response of a composite titania thin film with single-crystalline rutile nanorods embedded in anatase aggregates, J. Phys. Chem. C 112 (2008) 19484–19492.
[31] X.M. Song, J.M. Wu, M. Yan, Distinct visible-light response of composite films with CdS electrodeposited on TiO_2 nanorod and nanotube arrays, Electrochem. Commun. 11 (2009) 2203–2206.